ELSEVIER

Thin Solid Films 360 (2000) 268–273

thin solid films

www.elsevier.com/locate/tsf

Electrical properties of Ta_2O_5 thin films deposited on Cu

S. Ezhilvalavan[1], Tseung-Yuen Tseng*

Department of Electronics Engineering and Institute of Electronics, National Chiao Tung University, Hsinchu 300, Taiwan

Received 11 February 1999; received in revised form 15 September 1999; accepted 13 October 1999

Abstract

The electrical and dielectric properties of reactively sputtered Ta_2O_5 thin films with Cu as the top and bottom electrodes forming a simple metal insulator metal (MIM) structure, Cu/Ta_2O_5/Cu/n-Si, were studied. Ta_2O_5 films subjected to rapid thermal annealing (RTA) at 800°C for 30 s in N_2 ambient crystallized the film, decreased the leakage current density and resulted in reliable time-dependent dielectric breakdown characteristics. The conduction mechanism at low electric fields (<100 kV/cm) is due to Ohmic conduction; however, the Schottky mechanism becomes predominant at high fields (>100 kV/cm). Present studies demonstrate the use of Cu as a potential electrode material to replace the conventional precious metal electrodes for Ta_2O_5 storage capacitors. © 2000 Elsevier Science S.A. All rights reserved.

Keywords: Electrical properties; Copper; Tantalum; Oxides

1. Introduction

New capacitor dielectric materials with high dielectric constants are needed for advanced dynamic random access memory (DRAM) cell technologies if they are to keep up with the scaling rule. Ta_2O_5 thin film capacitors are considered as one of the best alternatives to conventional ultra-thin silicon dioxide which has reached its physical limits below 4 nm, or other thin film insulators such as oxide–nitride–oxide structures in terms of good dielectric properties [1–3]. As the DRAM generation goes 256 Mbit and beyond, the DRAM fabrication process has become more and more complicated. This will cause the production cost of the high density DRAMs to become unacceptably high and will significantly degrade the device reliability. Thus it is essential to develop a process technology that is simple and yet ensures high performance and high reliability.

In order for ultra large scale integrated circuit (ULSI) manufacturing to minimize the cost of ownership aspect in the metallization process, several metallization technologies have been proposed. The evidential criteria in choosing the most probable methods are physical or material limitations (e.g. step-coverage and resistivity) and manufacturing requirements such as process complexity, reliability, throughput and total cost.

Matsuhashi et al. [4] investigated the effects of top electrode materials, metals (W, Mo, Ti and Ta) and their nitrates (WN, MoN, TiN and TaN) on the leakage current in Ta_2O_5 films before and after annealing and proposed Mo and MoN as better electrodes for high temperature processes. Poly-Si, Pt, TiN and W have been evaluated as bottom electrodes for Ta_2O_5 dielectric films [5]. It was reported that TiN and W bottom electrodes had interfacial oxide layers which are smaller in thickness than that of the Si electrode, whereas Pt does not show any appreciable formation of an interfacial layer. The presence of an interfacial SiO_2 layer is responsible for the reduction of the dielectric constant in polycrystalline Ta_2O_5 films [6]. A poly-Si/TiN double layer was also introduced as an upper electrode in Ta_2O_5 capacitors where TiN served as a barrier layer to prevent reaction between Ta_2O_5 and poly-Si electrode under high thermal budget [7]. The application of poly-Si/TiN double electrode however has to be limited to relatively simple capacitor structures because of inherent poor conformability. Cu based interconnect metallization technology could be incorporated into devices by the turn of this century owing to ease of processing and high reduction in production cost of DRAMs. Recently, there have been significant improvements in various elements of Cu metallization process technology, including improved material properties, diffusion barriers, Cu deposition, Cu integration etc. Successful fabrication of semiconductor devices with good electrical performance, integrated with copper metallization has been demonstrated by Awaya et al. [8]. Current generation interconnect materials are Al and Al–Cu alloy. They could be replaced in the future by Cu and Cu alloy. Cu is favorable as an intercon-

* Corresponding author. Fax: +88-6-35-724-361.
E-mail address: tseng@cc.nctu.edu.tw (T.Y. Tseng)
[1] Present address: Physics and Astronomy, Michigan State University, East Lansing, MI 48824-116, USA. evalavan@pa.msu.edu

0040-6090/00/$ - see front matter © 2000 Elsevier Science S.A. All rights reserved.
PII: S0040-6090(99)00873-1

nect material since the upper limit of the current density to prevent electromigration for Cu is 5×10^6 A/cm^2, whereas for Al it is 2×10^5 A/cm^2 [9]. In this paper we report the effect of Cu as a top and bottom electrode material on the electrical and dielectric properties of reactively sputtered Ta_2O_5 films for the first time. We also evaluated the possibility of using Cu as the top and bottom electrode material for ULSI storage capacitors.

2. Experimental

The n-type silicon wafer was cleaned by a standard cleaning process. The Cu bottom electrode on n-Si substrate with a thickness of 200 nm was deposited using a separate sputtering system. The Cu film was prepared at a fixed power of 80 mW and at a constant pressure of 10 mTorr with Ar as the sputtering gas. Ta_2O_5 films were deposited on the Cu/n-Si bottom storage node electrode by dc-magnetron sputtering from a high purity tantalum metal target (2.5 inch diameter). More details on the deposition technique may be found in [10,11]. The sputtering gas was 80% Ar and 20% O_2 mixture with a total pressure of 10 mTorr. During deposition, the chamber was first back filled with Ar gas and used to pre-sputter clean the target for at least 5 min. Then the Ar/O_2 gases were introduced into the chamber to reach a total pressure of 10 mTorr. Film thickness was estimated to be 100 nm using a Tencor Alpha-step 200 profilometer. The Cu top electrode with a thickness of 200 nm and diameters of 150, 250 and 350 μm were patterned by a shadow mask process. The current–voltage (*I–V*) characteristics of the Ta_2O_5 films were measured on the MIM structure with a HP4145B semiconductor parameter analyzer. The capacitance–voltage (*C–V*) characteristic and the dielectric loss tangent were recorded at frequencies ranging from 100 Hz to 1 MHz with 0.5 V ac sweeping signal using a HP4194A impedance-gain phase analyzer. The rapid thermal annealing (RTA) of the Ta_2O_5 film was performed in a RTA furnace (Ulvac Sinku-Rico, HPC 700) at 800°C for 30 s in N_2 ambient, before the formation of the top electrode. The heating rate used was the maximum heating rate of about 100°C/s. Crystalline phases of the Ta_2O_5 films were identified by X-ray diffractometry (XRD, model D5000, Siemens, Munich, FRG).

3. Results and discussion

Fig. 1 shows the XRD patterns of as-deposited and Ta_2O_5 films subjected to RTA at 800°C for 30 s in N_2 ambient. XRD results indicate that as-deposited films were amorphous and the annealed films crystallized into β-Ta_2O_5. The crystallinity increased with temperature in terms of an increase in the intensity of the diffracted peaks, while the thickness of the film was kept constant. In addition, Fig. 1 also indicates the appearance of additional peaks corresponding to Cu (from the bottom electrode) and Cu_2O. The presence of Cu_2O peaks is due to the formation of an interfacial Cu_2O layer at the Ta_2O_5/Cu interface. However, the intensities of Cu_2O peaks decreased after the RTA N_2 annealing at 800°C. Ellipsometry measurements show that the refractive index (*n*) for the N_2 annealed Ta_2O_5 ($n = 2.239$) was higher than that of as-deposited Ta_2O_5 ($n = 2.149$). The thickness of as-deposited Ta_2O_5 was close to 100 nm and was reduced by ~2.5% after crystallization. Since we expect that $\Delta n/n$ is proportional to $\Delta\rho/\rho$ (where ρ denotes the density) through the Lorentz–Lorentz formula [12], the proximity of the variations observed is satisfying ($\Delta n/n \sim 4\%$) and confirms the hypothesis of densification induced during crystallization.

Fig. 2a,b depicts the relative counts of Cu and O atoms obtained from the X-ray photoelectron spectroscopy (XPS) analyses performed on the surfaces of as-deposited and N_2 annealed Cu bottom electrode deposited on Si substrate. The samples for the XPS analyses were prepared as follows in order to keep the exact surface conditions of the Cu bottom electrode as used during the deposition of Ta_2O_5 films, so that the formation or reduction of Cu_2O layer at the Ta_2O_5/Cu interface can be envisaged. Ta_2O_5 films were sputtered onto the as-deposited Cu bottom electrode for 5 min to form a very thin layer of Ta_2O_5 of thickness $\leq$10 nm. One of these samples was subjected to 800°C N_2 RTA for 30 s. Then, both the samples were ion etched for repeated cycles until the top Ta_2O_5 layer was removed completely and XPS analyses were performed on the freshly exposed as-deposited and N_2 annealed Cu bottom electrode on Si. We observed similar XPS spectra for the detected signal of Cu photoelectron, Cu($2p_{3/2}$), from the outermost surface of both as-deposited and N_2 annealed Cu bottom electrodes (Fig. 2a). The peak position for Cu($2p_{3/2}$) was detected at

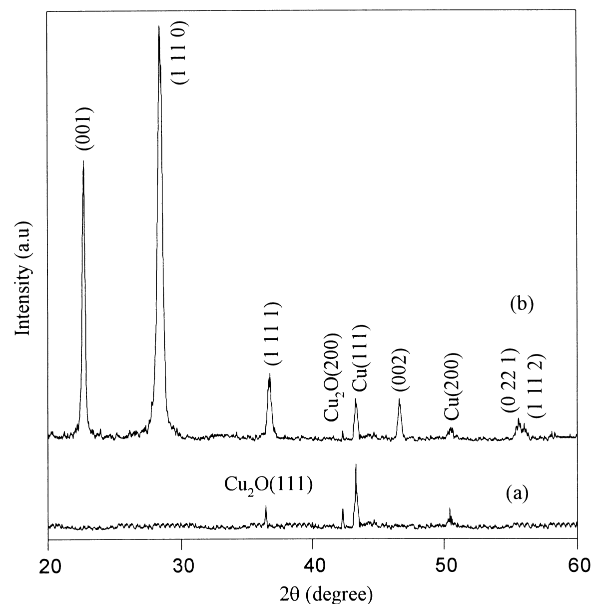

Fig. 1. XRD spectra of Ta_2O_5 film deposited on Cu: (a) as-deposited and (b) RTA processed at 800°C for 30 s in N_2 ambient.

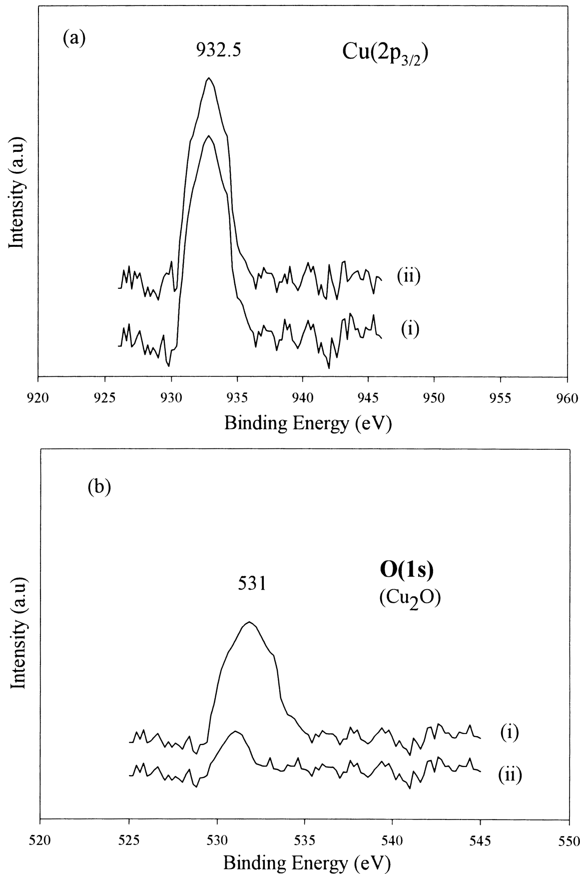

Fig. 2. XPS spectra of Cu bottom electrode: (a) Cu ($2p_{3/2}$) and (b) O (1s); (i) as-deposited and (ii) RTA processed at 800°C for 30 s in N_2 ambient.

932.5 eV as compared to the standard value of 932 eV, which indicates that the Cu bottom electrode preserved a high degree of Cu-elemental chemical state. The O(1s) spectra presented in Fig. 2b showed that the oxygen photoelectrons were in the Cu_2O state. The O(1s) peak position located at ~531 eV compares with the standard value. It is to be noted that the peak intensity of the O(1s) signal was decreased drastically for the N_2 annealed Cu bottom electrode in comparison to the as-deposited Cu bottom electrode. Therefore, XPS and X-ray analyses clearly demonstrate that the formation of Cu_2O took place mostly during the initial stages of Ta_2O_5 reactive sputtering, which was then dissociated when the films were subjected to N_2 annealing at 800°C for 30 s.

One of the most important features for a material to be used as an alternative storage dielectric in DRAM is the low leakage current density. Fig. 3 shows the *I–V* characteristics of the Ta_2O_5 thin film MIM capacitors as deposited and RTA processed at 800°C for 30 s in N_2 ambient. It is clear that the leakage current of as-deposited amorphous Ta_2O_5 film is larger than that of RTA processed polycrystalline film. The leakage current density of the as-deposited film is $\sim 10^{-4}$ A/cm^2 at 100 kV/cm which is brought down by nearly 4 orders to 10^{-8} A/cm^2 by RTA processing. This value falls in the middle of the leakage current densities recently reported for Ta_2O_5 films, which range from 10^{-7} A/cm^2 [13] to 10^{-11} A/cm^2 [14]. The reduction of leakage current after the 800°C 30 s N_2 RTA process might be closely related to the decrease in defects such as broken bonds and improvement in the film microstructure by way of higher densification. The as-deposited film could form an oxidized layer at the bottom electrode/Ta_2O_5 interface during initial stages of Ta_2O_5 reactive sputtering, which might be reduced during the 30 s 800°C N_2 RTA processing, as evident from X-ray and XPS results, yet preserving lower oxygen vacancy in the film, thereby restoring the leakage current density to $\sim 10^{-8}$ A/cm^2.

The oxidation of Cu bottom electrodes can be explained in terms of oxygen deficiency as a result of the reaction between the substrates and the adsorbed oxygen as follows. If the adsorbed oxygen molecules or radicals react with the substrate fast enough to remove the possibility of oxidation from the Ta source, Ta_2O_5 cannot be formed. As the surface oxide becomes thicker the diffusion flux of oxygen into the substrate becomes smaller, which alters the sputtered Ta ions to react with oxygen to form Ta_2O_5. Once the Ta_2O_5 film starts to grow, the oxidation of the substrate is actually stopped and the thickness of the interfacial oxide layer remains constant, because Ta_2O_5 film is an effective diffusion barrier material against oxygen [15].

The leakage current in a dielectric film can be owing to several conduction mechanisms including Schottky emission, Poole–Frenkel emission, Fowler–Nordheim tunneling and a space charge limited current. Herein, the leakage current mechanisms of Cu/Ta_2O_5/Cu/n-Si capacitors are investigated as well. Fig. 4 shows the Schottky emission (SE) plot for the as-deposited and the RTA processed Ta_2O_5 films. Two distinct regions may be observed in the *I–V* characteristic plotted in the form $\log_{10}(J)$ versus $E^{1/2}$. At

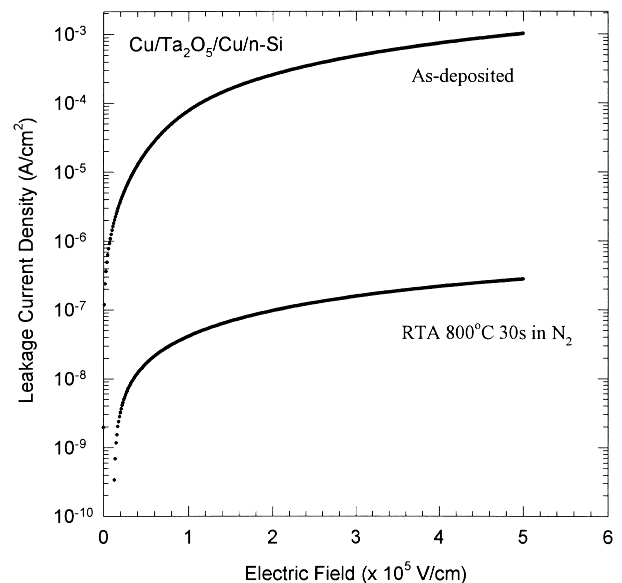

Fig. 3. *I–V* characteristics of the Ta_2O_5 films, as-deposited and RTA processed at 800°C for 30 s in N_2 ambient.

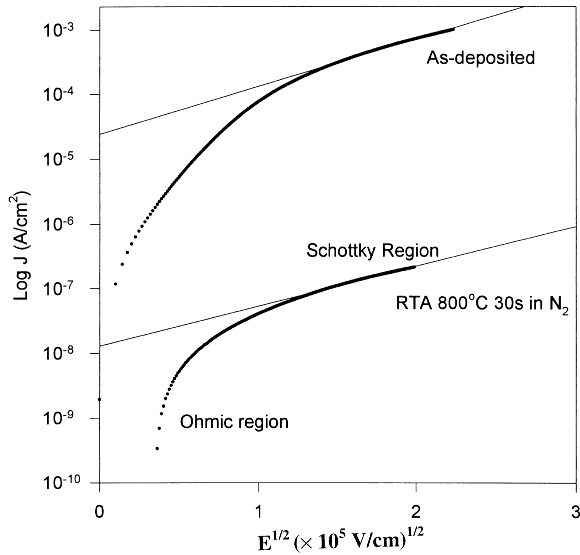

Fig. 4. Schottky plot for the as-deposited and RTA processed Ta_2O_5 films.

very low electric field the current density increases approximately linearly with the electric filed displaying nearly Ohmic behavior. Also a plot of I versus V (Fig. 5) indicates that for very low electric fields, 0–100 kV/cm, the relationship is Ohmic [16]. At higher electric fields and higher current densities, the I–V relationship is no longer Ohmic. It shows a non-linearity and the currents become quadratic with voltage [16]. Fig. 6 shows the Arrhenius plot of temperature dependent leakage current for RTA processed Ta_2O_5 film. It demonstrates two distinct slopes, i.e. a low activation energy process at low temperatures (suggesting electron hopping from one trap to the other with low mobility [17,18]), and a high activation energy mechanism at higher temperatures. The activation energies calculated from the measured slopes at low and higher temperatures are 0.08 eV and 0.39 eV respectively. It is also to be noticed that the current density of the film varies with temperature nearly in the form of $J \propto 1/T^{1/4}$, at lower temperatures and low fields, thus demonstrating the existence of hopping conduction [16–19]. Therefore, the current at lower electric fields (<100 kV/cm) in Fig. 4 could be due to hopping conduction, because the thermal excitation of the trapped electrons from one site to the other dominate transport in the film; this is given by [19]

$$J = \sigma E \exp\left(-E_a/KT\right) \tag{1}$$

where E_a is the activation energy of hopping electrons. But at higher electric fields >100 kV/cm (Fig. 4), the current densities are proportional to the square root of the applied electric field which extend further with the field. Furthermore, we were able to fit the current density variation at higher electric field in the form of a straight line, as indicated in Fig. 4, which satisfies the SE process. The linear relation at higher electric field demonstrates the dominance of SE process across the interface between the dielectric film and the electrode as a result of barrier lowering due to the applied field and the image force [10,14,16]. The current (J_{SE}) governed by the SE mechanism is described as [19]

$$J_{SE} = AT^2 \exp\left[-q\left(\phi_b - \left(qV/4\pi\epsilon_i d\right)^{1/2}/KT\right)\right] \tag{2}$$

where A denotes a constant, ϕ_b the Schottky barrier height, ϵ_i the dielectric constant of the insulator, V the applied voltage and d the insulator thickness. The comparison of calculated dielectric constant from the slope of the straight line portion of the SE plot with the experimentally determined (from C–V measurement at 100 kHz) value further confirmed the existence of the SE process for the present films. In the $Cu/Ta_2O_5/Cu/n$-Si structure, electrons are injected from n-Si into Cu when the top electrode is positively biased. Since the work functions of Ta_2O_5 and Cu are 4.05 eV [20] and 4.7 eV [20] respectively, the barrier height at the Cu/Ta_2O_5 interface is smaller than that of the normally used Pt/Ta_2O_5 interfaces (because of the higher work function of Pt ~5.65 eV [20]). Therefore, for the same applied fields ≥100 kV/cm, the number of electrons injected from the Cu/Ta_2O_5 interface into the dielectric film is higher than that from the Pt/Ta_2O_5 interface. In other words, the leakage current in the Ta_2O_5 film increases with decreased work function of the top electrode. This result indicates that the current flowing through the Cu/Ta_2O_5 interface is limited by the SE process. Thus the I–V characteristics clearly demonstrate the existence of two possible dominant conduction mechanisms for $Cu/Ta_2O_5/Cu/n$-Si MIM capacitors. The problem of higher leakage current density in Ta_2O_5 films with the use of Cu as an electrode can be improved by carrying out the N_2 RTA processing at 800°C for 30 s after the deposition of the top electrode. It has been reported that annealing the dielectric film $(Ba,Sr)TiO_3$ with both top and bottom electrodes in reducing atmosphere (N_2) creates an n-type conductivity in the dielectric film and produces a high interface energy barrier, which plays a major role in reducing the current density when the bias voltage is applied

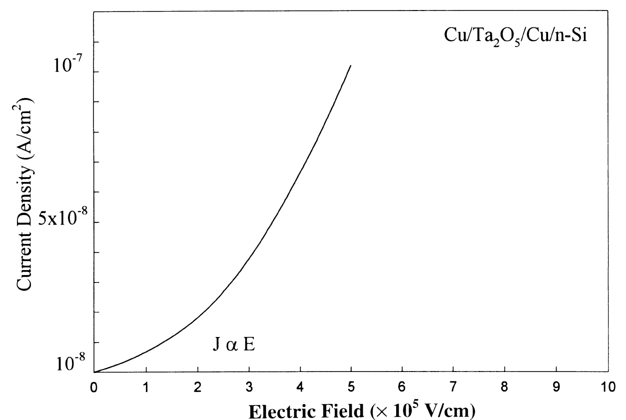

Fig. 5. Current–voltage plot of leakage current in RTA processed $Cu/Ta_2O_5/Cu/n$-Si capacitor.

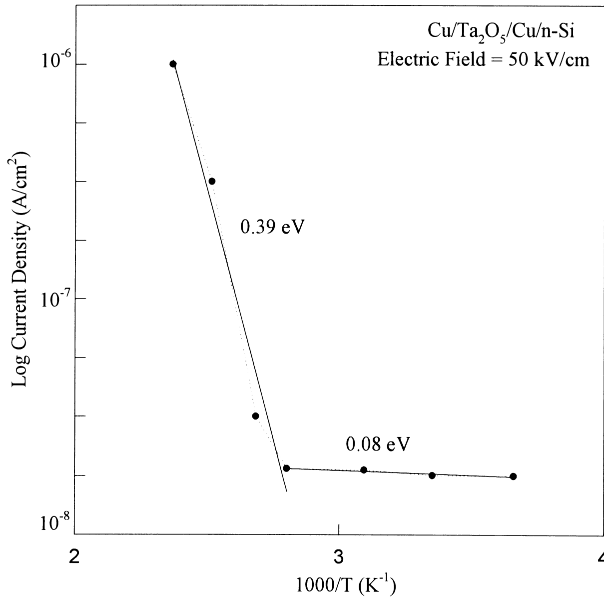

Fig. 6. Arrhenius plot of temperature dependent leakage current for Ta_2O_5 film RTA processed at 800°C for 30 s in N_2 ambient.

[21]. Hence we can imagine that the decreased work function of the top electrode may not be a disadvantage in using Cu as an electrode in dielectric films.

Fig. 7a,b displays the results of the dielectric studies performed on the $Cu/Ta_2O_5/Cu/n-Si$ MIM configuration. It shows the variation of accumulation capacitance as a function of logarithmic frequency (a) for the as-deposited Ta_2O_5 film and (b) for a Ta_2O_5 film RTA processed at 800°C for 30 s in N_2 ambient, for frequencies ranging from 100 Hz to 1 MHz. The capacitance of the as-deposited film decreased from 1.0 F/m^2 at 100 Hz to 2×10^{-3} F/m^2 at 1 MHz and the dielectric loss tangent falls from a high value of 12 at 100 Hz to 1 at 1 MHz. The capacitance of the RTA processed film, however, shows less variation with frequency, i.e. it falls from 4.6×10^{-3} F/m^2 at 100 Hz to 3.1×10^{-3} F/m^2 at 1 MHz. The loss tangent is a fairly low value and it varies from 0.06 to 0.01 in the above measured frequency range. The dielectric constants of the as-deposited and the RTA processed Ta_2O_5 films calculated from the capacitance measured at 100 kHz are 30 and 40, respectively. The presented dielectric constant is higher than that reported in the literature [14,16]. This difference may be attributed to the differences in the processing methods, processing temperature and ambient and also in the resultant structure-phase modifications. The large capacitance variation and the associated higher dielectric loss tangent at low frequencies for the as-deposited films may be attributed to the higher leakage current density. The RTA processing at 800°C for 30 s leads to complete crystallization and higher densification resulting in lower leakage current density, which may be the probable reason for the low dielectric loss tangent of the polycrystalline film. Furthermore, RTA processing in N_2 ambient provides a reducing interface for the oxidized surface layer of the Cu electrode, yet preserving a lower oxygen vacancy concentration in the dielectric film. The reason is that the value of the formation energy of Ta_2O_5 at 800°C (−597 kJ/mol) [20] is much more negative than that of Cu_2O (−60 kJ/mol) [20], therefore the dissociation of oxygen from the Ta_2O_5 film is less probable than from Cu_2O during the short duration (30 s) of the RTA processing in N_2.

Time-dependent dielectric breakdown (TDDB) is a characteristic of the intrinsic materials, the method of processing and electrode materials. Fig. 8 shows the lifetime extrapolation from the dependence of the cumulative failure on TDDB stress time for RTA processed $Cu/Ta_2O_5/Cu/n-Si$ thin films. The TDDB lifetime for Ta_2O_5 film with the conventional Pt electrode MIM structure is also shown for comparison [14]. Present studies demonstrate that Ta_2O_5 MIM films with Cu as the top and bottom electrode can also survive the 10 years lifetime at a stress field of ≥700 kV/cm. However, we believe that more optimal conditions of RTA processing in N_2 are required to improve the $Cu/Ta_2O_5/Cu/n-Si$ capacitor performance. The details have to be separately worked out.

4. Conclusion

We have successfully demonstrated the effective use of Cu as a possible electrode material replacing the conventional precious metal electrodes for Ta_2O_5 film storage capa-

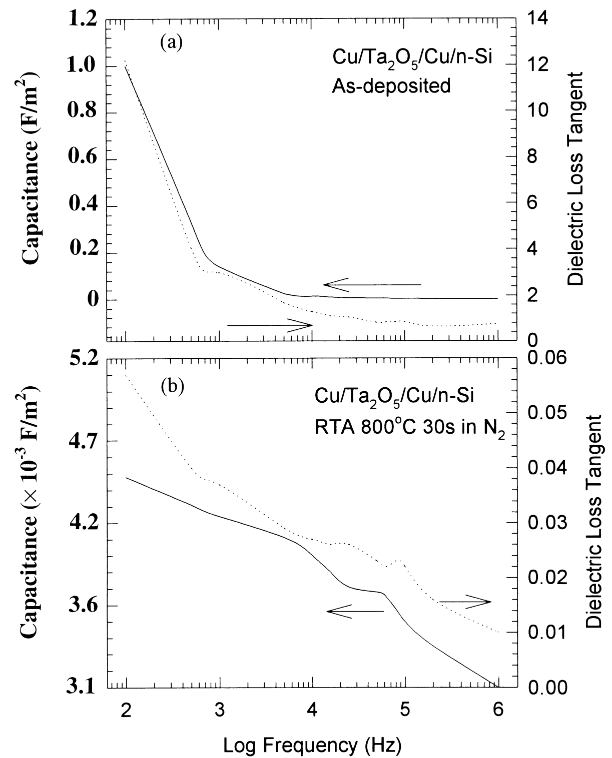

Fig. 7. Capacitance as a function of logarithmic frequency for the Ta_2O_5 film: (a) as-deposited and (b) RTA processed film.

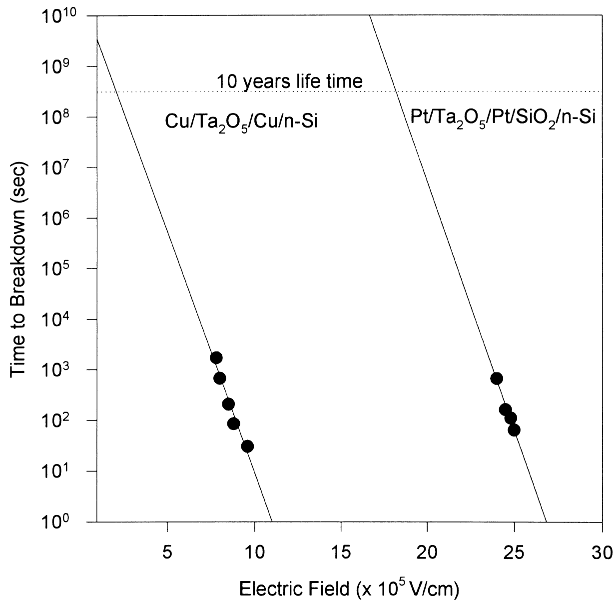

Fig. 8. TDDB lifetime as a function of electric field for Ta_2O_5 films.

citors. Usage of Cu as an electrode will significantly reduce the production cost of future high density DRAMs.

Acknowledgements

The authors gratefully appreciate the financial support from the National Science Council of R.O.C under project no. NSC 87-2218-E 009-008.

References

[1] S. Kamiyama, H. Suzuki, H. Watanabe, et al., IEDM Tech. Dig. (1993) 49.
[2] H. Shinriki, M. Nakata, IEEE Trans. Electron Devices 38 (1991) 455.
[3] F.C. Chiu, J.J. Wang, J.Y. Lee, S.C. Wu, J. Appl. Phys. 81 (1997) 6911.
[4] H. Matsuhashi, S. Nishikawa, Jpn. J. Appl. Phys. 33 (1994) 1293.
[5] I. Kim, J.S. Chun, W.J. Lee, Mater. Chem. Phys. 44 (1996) 288.
[6] S. Shinriki, Y. Nishioka, Y. Ohji, K. Mukai, IEEE Trans. Electron. Devices 36 (1989) 328.
[7] M.B. Lee, H.D. Lee, B.L. Park, U.I. Chung, Y.B. Koh, M.Y. Lee, IEDM Tech. Dig. (1996) 683.
[8] N. Awaya, H. Inokawa, E. Yamamoto, et al., IEEE Trans. Electron Devices 43 (1996) 1206.
[9] A.R. Sethuraman, J.F. Wang, L.M. Cook, Semicond. Int. 6 (1996) 177.
[10] S. Ezhilvalavan, T.Y. Tseng, J. Appl. Phys. 83 (1998) 4797.
[11] S. Ezhilvalavan, T.Y. Tseng, J. Am. Ceram. Soc. 82 (1999) 600.
[12] C.P. Smyth, Dielectric: Behaviour and Structure, McGraw-Hill, New York, 1955.
[13] G.Q. Lo, D.L. Kwong, P.C. Fazan, V.K. Mathews, N. Sandler, Electron Devices Lett. 14 (1993) 216.
[14] S. Zaima, T. Furuta, Y. Koide, Y. Yasuda, J. Electrochem. Soc. 137 (1990) 2876.
[15] T. Kato, T. Ito, J. Electrochem. Soc. 135 (1988) 2586.
[16] S. Banerjee, B. Shen, I. Shen, J. Bohlman, G. Brown, R. Doering, J. Appl. Phys. 65 (1989) 1140.
[17] P.L. Young, J. Appl. Phys. 47 (1976) 235.
[18] C.A. Mead, Phys. Rev. 128 (1962) 2088.
[19] J. O'Dwyer, Theory of Electrical Conduction and Breakdown in Solid Dielectrics, Clarendon, Oxford, 1973.
[20] D.R. Lide, CRC Handbook of Chemistry and Physics, CRC Press, Boston, MA, 1991.
[21] C.S. Hwang, S.O. Park, H.J. Cho, C.S. Kang, H.K. Kang, S.I. Lee, M.Y. Lee, Appl. Phys. Lett. 67 (1995) 2819.